Journal of Statistical Physics, Vol. 110, Nos. 3–6, March 2003 (© 2003)

Computations of Dendrites in 3-D and Comparison with Microgravity Experiments

Y. B. Altundas[1] **and G. Caginalp**[1]

Received September 27, 2001; accepted February 28, 2002

The phase field model is used to compute numerically the temporal evolution of the interface for solidification of a single needle crystal of succinonitrile (SCN) in a three dimensional cylindrical domain with conditions satisfying microgravity experiments. The numerical results for the tip velocity are (i) consistent with the experiments, (ii) compatible with the experimental conclusion that tip velocity does not increase for larger anisotropy (e.g., for pivalic acid), (iii) different for 3D versus 2D by a factor of approximately 1.76, (iv) strongly dependent on physical value of the kinetic coefficient in the model. Also, as indicated by theory and the laboratory experiments, the results obtained for single needle crystal show that the growth velocity approaches a constant value in large time.

KEY WORDS: Solidification; phase field equations; dendrite; single needle crystal; succinonitrile; microgravity.

The temporal evolution of an interface during solidification has been under intensive study by physicists and material scientists for several decades. The interface velocity and shape have important consequences for practical metallurgy, as well as the theory, e.g., velocity selection mechanism and nonlinear theory of interfaces. The simplest observed microstructure is the single needle crystal or dendrite, which has been modeled in an early study by Ivantsov[(1)] as a paraboloid growing at a constant velocity, v_0, with tip radius, R_0, subject to the heat diffusion equation and latent heat considerations at the interface. With the interface stipulated to be at the melting temperature, the absence of an additional length scale implies the existence

[1] Mathematics Department, University of Pittsburgh, Pittsburgh, Pennsylvania 15260; e-mail: {ybast,caginalp}@pitt.edu

0022-4715/03/0300-1055/0 © 2003 Plenum Publishing Corporation

of an infinite spectrum of pairs of velocities and tip radii, (v_0, R_0). Experimentally it has been observed that a unique pair (v_{exp}, R_{exp}) is selected, so that the tip velocity is constant throughout the experiment, and is independent of initial conditions.

The theoretical mechanism for this velocity selection has been the focus of much of the theoretical research on the subject (see, for example, refs. 2–6). The emergence of the capillarity length associated with the surface tension as an additional length scale has provided an explanation for the selection mechanism. Advances in computational power and a better understanding of interface models and their computation have opened up the possibility of comparing experimental values for the tip velocity with the numerical computations. This is nevertheless a difficult computational issue in part due to the large differences in length scales that range from 1 cm for the size of the experimental region, to 10^{-6} cm for the capillarity length, to 10^{-8} cm interface thickness length.

One perspective into the theoretical and numerical study of such interfaces has been provided by the phase field model introduced in refs. 7 and 8 in which a phase, or order parameter, ϕ, and temperature, T, are coupled through a pair of partial differential equations described below (see also more recent papers).[9, 10] In physical terms, the width of the transition region exhibited by ϕ is Angstroms. In the 1980's two key results facilitated the use of these equations for computation of physically relevant phenomena. If the equations are properly scaled one can (i) identify each of the physical parameters, such as the surface tension, and attain the sharp interface problem as a limit,[11, 12] and (ii) use the interface thickness, ε, as a free parameter, since the motion of the interface is independent of this parameter.[13] The latter result thereby opened the door to computations with realistic material parameters, by removing the issue of small interface thickness. However, the difference in scale between the capillarity length and overall dimensions still pose a computational challenge.

More recently, several computations, have been done using the phase field model,[14–21] with some 3D computations in refs. 15 and 16 utilizing the model of ref. 22, that will be compared with our results below.

In this paper we present computations that have the following novel features:

(A) We perform numerical computations for a cylindrical region in three dimensional space by utilizing rotational symmetry. This allows us to compare the tip velocity with the actual experiments in a meaningful way.

(B) The calculations utilize the parameters and boundary conditions of the IDGE microgravity experiments for succinonitrile (SCN).[23] All previous experiments done under normal gravity conditions involved

convection. Hence this provides the first opportunity to compare experiments in the absence of convection to theory that also excludes convection. Our results for tip velocity compare favorably with the data of these experiments.

(C) The role of anisotropy in velocity selection has been noted in the computational references cited above. Glicksman and Singh[24] compare experimental tip velocities of SCN with pivalic acid (PVA) whose coefficients of surface tension anisotropy (defined below) differ by a factor of 10 but are otherwise similar, except perhaps for the kinetic coefficient. The graph of their data (ref. 24, Fig. 7) indicates that the tip velocities of the two materials differ by less than 10 percent.

We perform two sets of calculations in which all parameters are identical (SCN values) except for the anisotropy coefficient. Our computations confirm (consistent with the experimental results[24]) that the velocities are nearly identical when the magnitude of the anisotropy is varied by a factor of 10 with all other parameters fixed (at the SCN values).

Researchers using solvability theory[2–6] have maintained that the presence of anisotropy in the governing equations is necessary in order to select the appropriate tip velocity. The fact that this tip velocity does not appear to change much as the magnitude of anisotropy is increased appears to be consistent with solvability theory.

(D) Most of the previous numerical computations that simulate the interface growth were done in 2D. Our computations shows that the 2D and 3D computations differ by a factor of approximately 1.76.

(E) The role of the kinetic coefficient (see definition of α below Eq. (1b)) is subtle, and this material parameter is often set to zero, for convenience, in theoretical and computational studies. We find, however, that there is a significant difference in the tip velocity when all other parameters are held fixed while this coefficient is varied.

Consequently, this kinetic coefficient may be of crucial importance in determining the selection of tip velocity. A better understanding of this issue may lead to theory that can explain a broader range of undercooling and velocities.

Our findings also have implications in terms of computations using variations on phase field models that either set the kinetic coefficient to zero or introduce artificial kinetic terms. This suggests that further experiments and theory on this subject may lead to a deeper understanding of dendritic phenomena. In the computations below we use a version of the phase field equations introduced in ref. 22, for which the phase or order parameter, $\phi(\vec{x}, t)$, as a function of spacial point, x, and time, t, is

exactly -1 in the solid and $+1$ in the liquid. We define the dimensionless temperature, u, and the capillarity length, d_0, by

$$u(x, t) = \frac{T - T_m}{l_v / c_v}, \qquad d_0 = \frac{\sigma c_v}{[s]_E \, l_v}$$

where T_m, l_v and c_v are the melting temperature, latent heat and specific heat per unit volume of the material, respectively. Thus, we write the dimensionless phase field equations as following.

$$u_t + \tfrac{1}{2}\Phi_t = D\,\nabla^2 u \tag{1a}$$

$$\alpha\varepsilon^2\phi_t = \varepsilon^2\,\nabla^2\phi + g(\phi) + \frac{5\varepsilon}{8d_0}\,u f'(\phi) \tag{1b}$$

where

$$g(\phi) = \frac{(\phi - \phi^3)}{2}, \qquad f'(\phi) = (1-\phi^2)^2, \qquad D = \frac{K}{c_v}$$

and the interface is defined by $\Gamma = \{x \in \Omega : \phi(x, t) = 0\}$. Here α is the kinetic coefficient and ε is the interface thickness that can be used as a "free parameter."[13] In the limit as ε vanishes as all other parameters held fixed, solutions to (1a) and (1b) are governed by the sharp interface model

$$u_t = D\,\nabla^2 u \qquad \text{in } \Omega - \Gamma(t) \tag{2a}$$

$$v_n = D\,\nabla u \cdot \hat{n}_+^- \qquad \text{in } \Gamma(t) \tag{2b}$$

$$u = -d_0\kappa - \alpha\, d_0 v_n \tag{2c}$$

where the parameters d_0, D, α are the same as in (1a) and (1b), and v_n is the interface growth velocity (with normal chosen from solid to liquid).[7, 22]

In order to simulate the interfacial growth of a 3D single needle dendrite for the compound succinonitrile (SCN) in a cylindrical geometry (under the assumption that the needle grows symmetrically), we consider a domain which is a cylindrical chamber filled with the pure melt. A small radially symmetric seed is placed at the bottom center of the chamber. We denote the flat surface of the cylinder where the seed is placed by S_1, the flat surface across from the seed (i.e., far field) by S_2, and the curved surface around the cylinder by S_3. Thus we define the boundary and initial conditions below as follows. The temperature at S_2 and S_3 are kept at the constant undercooling value u_∞. The temperature at S_2 is also kept at a constant (in time) temperature, but declines exponentially from $u = 0$ on the interface of the seed to the intersection of S_2 with S_3, where $u = u_\infty$.

In particular, the boundary condition for u on S_2 is given as $u_{\text{trav}}(s, 0)$ where s is the distance from the seed interface, and

$$u_{\text{trav}} = \begin{cases} u_\infty(1-\exp\{-v(z-vt/|u_\infty|)/(D|u_\infty|)\}) & z > vt/|u_\infty| \\ 0 & z \leqslant vt/|u_\infty| \end{cases} \tag{3}$$

is a plane wave solution to a 1-D problem. The order parameter is initially set to its equilibrium value

$$\phi(\rho) = \tanh((\rho - vt)/(2\varepsilon)) \tag{4}$$

where ρ is the signed distance (positive in the liquid) from the interface.[22] The boundary conditions for ϕ are defined to be compatible with those on the temperature.

The anisotropy is incorporated into the equations through the surface tension where one has precise and quantitative experimental data in order to utilize the experimentally observed quantities and parameters. Thus, we write the surface tension as

$$\sigma(\theta) = \sigma_0[1 + \delta_\sigma \cos(M(\theta - \theta_0))] \tag{5}$$

where M is an integer, $\delta_\sigma \in \mathrm{R}^+$ and θ_0 are the amplitude of the anisotropy and the preferred angle, respectively. The variable θ in (5) is defined to be the angle between the normal to the interface and x-axis, i.e.,

$$\cos\theta = \frac{\vec{\nabla}\phi}{|\nabla\phi|} \cdot \hat{x}$$

We suppress the second angle in the anisotropy in view of the cylindrical symmetry. Asymptotic analysis[25] shows that with anisotropy the generalized Gibbs–Thomson relation (2c) is modified not only in terms of an angle dependent surface tension, $\sigma(\theta)$, but with its second derivative as well so that (2c) becomes

$$u = -d_0(\theta)\,\kappa - \alpha\, d_0(\theta)\, v_n \tag{2c'}$$

where, now, the relationship between σ and d_0 is given by

$$d_0(\theta) = \frac{\sigma(\theta) + \sigma''(\theta)}{[s]_E\, l_v}\, c_v$$

Hence, if $(M_2 - 1)\,\delta_\sigma < 1$ is satisfied then the curvature has its maximum at $\theta = \theta_0$.[13] This is consistent with the experimental evidence.[24]

For computational convenience, we take a vertical cross section through the origin. Upon writing the Eqs. (1a) and (1b) in cylindrical coordinates, the terms involving θ drops out and we get a simplified form of the phase field equations in a cylindrical coordinate system.

We use a semi-implicit Crank–Nicolson finite difference method to discretize the equations by lagging the nonlinear terms in (1b). The singularity at $r = 0$ is avoided by using the operator value $\frac{\partial^2}{\partial r^2}$ as an approximation for $\frac{1}{r}\frac{\partial}{\partial r}$ at r=0 only.[26] The motivation for this approximation is that both $\frac{\partial \phi}{\partial r}$ and $\frac{\partial u}{\partial r}$ are zero at $r = 0$.

An adequate number of mesh points on the domain are necessary for the accurate computation of ϕ in the interfacial region, which is costly since the mesh size has a strong influence on the speed and size of the computation. We lay $L \times L$ uniform mesh points over the domain such that at least 6 or 7 grid points are located at the interfacial region as measured from $\phi = -0.9$ to $\phi = 0.9$. Throughout computations for each undercooling value, we set $L = 600$.

Using the undercooling value $\Delta u = 0.01$, we performed computations for different choice of grid sizes to test the grid convergence. Table I shows the corresponding velocities for $L = 200$, 300, 400, 500, 600 and 700 when all other conditions are identical. Of course, the grid sizes smaller than 400 result in an interface width that is unrealistic, but we have an excellent convergence as shown by the values of $L = 600$ and $L = 700$.

The measured values of d_0, D and σ_0 for SCN are given by 2.83×10^{-7} cm, 1.147×10^{-3} cm ^{2}/s and 8.9 ergs/cm ^{2}, respectively.[27] We set the free parameter, ε, as h where $h = 1/L$ and the time step is $\Delta t = 5 \times 10^{-3}$. Under these conditions, one has $R_0 \sim 14h$ and the diffusion length, D/v_n, is at least 20 times larger than the tip radius, R_0, satisfying the standard

Table I. Computational Growth Velocities Corresponding to the Undercooling Value 0.01 of SCN. The Velocities Are Calculated at $t^* = 16$ s. From The Initial Stage for Each L when All Other Conditions Are Identical

L	Velocity (cm/s)
200	0.002100
300	0.000360
400	0.000304
500	0.000327
600	0.000342
700	0.000357

theoretical conditions for dendritic growth.[17] Moreover, we set $M = 4$ and $\theta_0 = \pi/2$ so that the solid protrudes further in the vertical and the horizontal directions in accordance with 4-fold symmetry.

Upon using (3) and (4) as initial conditions and the boundary conditions described above, semi-implicit finite difference discretization of the equations results with two systems of equations

$$A_\phi \phi = b_\phi \tag{6}$$

$$A_u u = b_u \tag{7}$$

where A_u and A_ϕ are the corresponding coefficient matrices, and b_u and b_ϕ are the right handside vectors for u and ϕ, respectively. Equations (6) and (7) are solved consecutively for each time stepping Δt by ITPACK2C which is a collection of subroutines written in Fortran programming language for solving large linear system of equations by adaptive accelerated iterative algorithms.[28]

In order to address the issue raised in (A) and (B) above we consider nine dimensionless undercooling values from the microgravity experiments (IDGE) for SCN.[23] The computations for 20 seconds confirm that there is a linear relation between the undercoolings and corresponding growth velocities (Figs. 1 and 2) for SCN. Table II shows that the computed results for velocity are close to the experimental values for each of the (dimensionless) undercooling values 0.00610, 0.0079, 0.01, 0.0126, 0.0161 and 0.0205 and outside of the experimental error range for the values 0.0265, 0.0338 and 0.0437. The results are consistent with other phase field studies that confirm this linear relation (see e.g., ref. 15)).

The tip radius is more difficult to measure accurately. We use the method of selecting six points on near the tip of the paraboloid and using a least squares procedure to select the optimal parabola. The radius of curvature can then be determined from this curve in an accurate way. The results are within a factor of three of the microgravity experiment measurements.

Next, we consider the issue discussed in (C) above. We note that other numerical studies involving anisotropy have usually assumed dynamical anisotropy. Here we use only the anisotropy that can be quantified from experiments, namely, the anisotropy of the surface tension, which is an equilibrium quantity. For the undercooling 0.01, we perform three computations for different δ_σ values of 0.005, 0.01 and 0.03 to determine the influence of anisotropy on the tip velocity [see Eq. (5)]. The corresponding growth velocities for each δ_σ are 0.000524, 0.000527 and 0.00054 (cm/s), respectively.

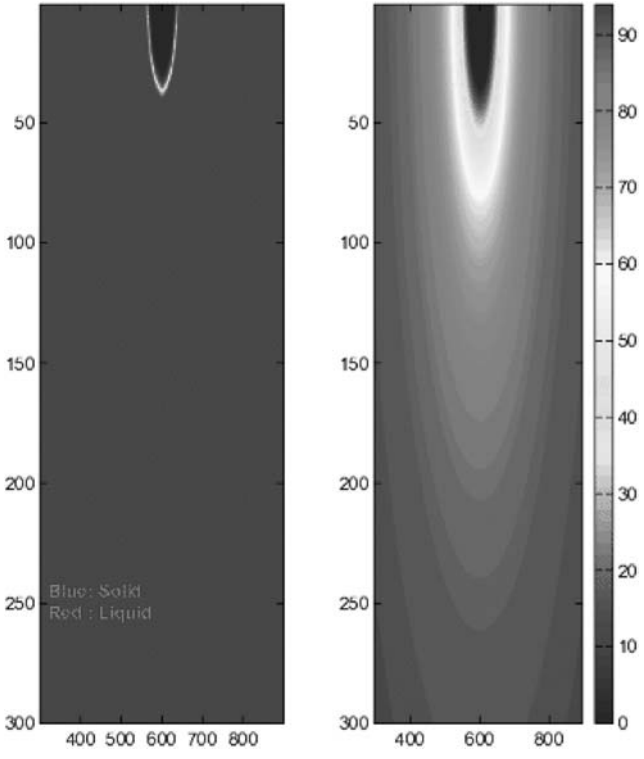

Fig. 1. The plots of the dendritic growth into melt for the supercooling 0.001; (a) shows the phase field, and (b) shows the temperature field after 100 s.

As mentioned earlier, the surface tension anisotropy for PVA is much larger than that of SCN. The experiments suggest that the tip velocity is similar for both materials. However, the possible difference in the kinetic coefficients between the two materials does not allow one to conclude that the magnitude of anisotropy does not influence the tip velocity. Our computational studies, on the other hand, indicate that an order of magnitude change in the anisotropy coefficient does not change the tip velocity significantly, confirming the stated conclusion of the experimenters.[24] Moreover the shape of the dendrite also does not appear to be effected very much. Only the tip of the dendrite becomes sharper for larger anisotropy, also confirming the experimental results.

The comparison of the growth velocities in 2D and 3D are examined for the undercoolings values of 0.01, 0.0161 and 0.0265. Since exactly the same initial and boundary conditions are used in both computations, the

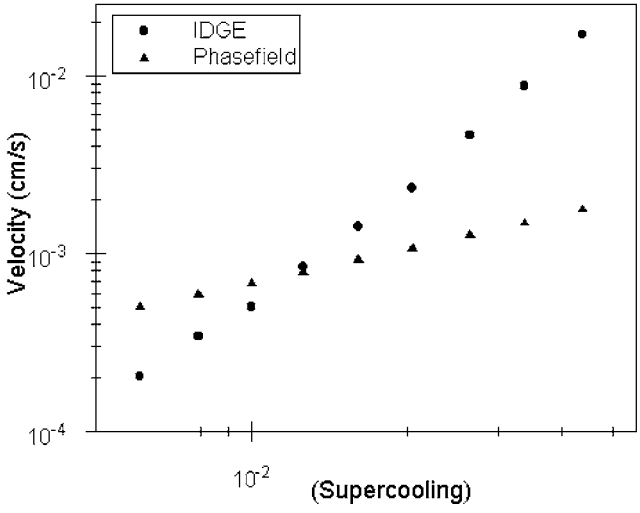

Fig. 2. Dimensionless supercooling versus growth velocities (Log scales).

tip velocities for 2D and 3D can be compared. The velocities corresponding to these undercoolings in 2D are 0.00033, 0.0005 and 0.00066 (cm/s), compared with the values of 0.00058, 0.00083 and 0.0012 (cm/s), respectively.

The ratio 1.76 can be put in perspective by examining the limiting sharp interface equations (2a) and (2b). Physical intuition suggests that the growth of the interface is limited mainly by the diffusion of the latent heat

Table II. Microgravity Dendritic Growth Velocity Measurements Calculated from Telemetered Binary Images from the Space Shuttle Colombia (STS-62) and Computational Velocities

Supercooling	Velocity (IDGE) (cm/s)	Velocity (Computational) (cm/s)
0.0437	0.01698	0.001770
0.0338	0.00872	0.001486
0.0265	0.00462	0.001273
0.0205	0.002328	0.001066
0.0161	0.001417	0.000922
0.0126	0.000840	0.000784
0.0100	0.000500	0.000681
0.00790	0.000343	0.000590
0.00610	0.000204	0.000502

manifasted in the condition (2b). When diffusion is rapid, the heat equation is approximated by Laplace's equation, whose radial solutions are of the form r^D. The latent heat condition (2b) implies that the normal velocity is proportional to the gradient, or Dr^{D-1}. Comparing this term for $D=3$ versus $D=2$, one has a ratio of $3/2=1.5$. Analogously, if we examine the Gibbs–Thomson relation alone, and solve (2c) for the normal velocity, we see that dimensionality arises (directly) in terms of κ, the sum of principal curvatures, which is $(D-1)/R_0$ where R_0 is the radius of curvature. Hence this factor would suggest that at least one of the terms in this expression for the velocity has a coefficient $D-1$, suggesting a ratio of $(3-1)/(2-1)=2$. Thus a heuristic examination of the key limiting equations suggests that the tip velocity in 3D should be about 1.5 to 2 times that of the 2D system. Of course there are numerous nonlinearities involved in the equations that could alter this ratio. Our calculations fall well in the range 1.5 to 2, thereby lending some support to the heuristics above.

As discussed above, the tip velocity of the dendrite has been the focus of much of the theoretical research known as "solvability theory" for many years.[2–6] This research has focused on the mechanism whereby a single velocity is selected from the infinite spectrum of possibilities that are obtained from Ivantov solutions as a consequence of additional length scale introduced by surface tension. The phase field computations have provided an independent method for computing this velocity and thereby checking the theory. The phase field computations of refs. 10 and 15 have demonstrated the consistency between the numerical computations and theory. In ref. 10 a number of variations of phase field equations are compared to the results of solvability theory. In each case, the phase field computations reach a steady state in which the tip velocity is constant. The computed velocities are within a few percent of the velocity predicted by solvability theory. The work of ref. 10 and earlier work[29] also show that the variations on the phase field equations (including those that claim a greater level of "thermodynamic consistency") are almost identical in terms of the computed result and time required for the computation.

Our calculations confirm that the single needle-crystal approaches a constant growth rate in a 3D computation. For example, using the dimensionless undercooling value of 0.01, the average growth velocity is calculated at nine different time steps from 10 to 110 s. The results show that the growth velocity approaches a constant value in large time (Fig. 3) as indicated in solvability theory and previous computational studies.[10]

Finally, we examine the role of the kinetic coefficient, discussed in (E) above, by varying α while other parameters are fixed. We use the undercooling $\Delta u = 0.01$ with the kinetic coefficients 1.5×10^6, 3.0×10^6 and 3.5×10^6 so that we could see the change in the growth velocity when the magnitude

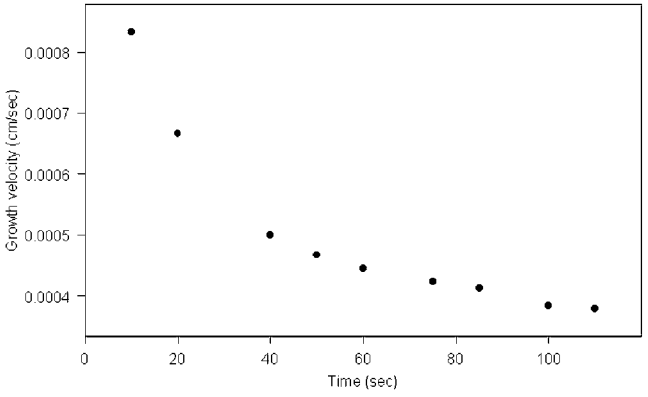

Fig. 3. Computational growth velocity versus time for the undercooling 0.01.

of kinetic coefficient is reduced from the value, 3.5×10^6, which is the value we used throughout our computations. The corresponding velocities for each α are 0.00016, 0.00066, and 0.00083 (cm/s). This indicates a strong dependence on this parameter which is a physically measurable quantity. Hence, setting this parameter to zero, which may be convenient from some perspectives (see e.g., refs. 15 and 16) appears to change the tip velocity significantly. This may be the reason for the conclusion in ref. 15, p. 4347, that "For PVA the agreement between theory and experiment remains very poor." In other words, the approximation $\alpha \approx 0$ is not valid for some materials. The material constants for PVA and SCN differ in the magnitude of the anisotropy and, perhaps, the kinetic coefficient, α. We have demonstrated that the magnitude of the anisotropy (when altered by almost an order of magnitude) does not have a strong influence on the tip velocity, while the kinetic coefficient (when altered by much less than an order of magnitude) has a dramatic influence. Thus, our calculations suggest that the kinetic coefficient is perhaps responsible for the lack of agreement between computations (or theory) versus experiment. At present there is little theoretical evaluation and experimental data for this parameter.[30] In all other experiments in this paper, we used a value of 3.5×10^6 which is obtained from (2c). Further experimental data on this parameter would be very useful for developing our understanding of dendritic phenomena.

ACKNOWLEDGMENTS

Supported by NSF Grant No. DMS-9703530 and by a grant from the Office of the Provost and Council on Academic Computing, The University of Pittsburgh. We are grateful for data provided by Dr. M. B. Koss.

REFERENCES

1. G. P. Ivantsov, Temperature field around spherical, cylindrical and needle-shaped crystals which grow in supercooled melt, *Dokl. Akad. Nauk USSR* **58**:567 (1947)
2. E. Ben, Jacob, N. Goldenfeld, B. Kotliar, and J. Langer, Pattern selection in dendritic solidification, *Phys. Rev. Lett*. **53**:2110 (1984)
3. D. A. Kessler, J. Koplik, and H. Levine, Geometric models of interface evolution. II Numerical Simulation, *Phys. Rev. A* **30**:3161 (1984)
4. D. A. Kessler, J. Koplik, and H. Levine, Pattern selection in fingered growth phenomena, *Adv. Phys*. **37**:255 (1988)
5. E. Brener and V. I. Melnikov, Pattern selection in two-dimensional dendritic growth, *Adv. Phys*. **40**:53 (1991)
6. Y. Pomeau and M. B. Amar, *Solids Far from Equilibrium*, C. Godreche, ed. (Cambridge University Press, Cambridge, England, 1991), p. 365
7. G. Caginalp, The limiting behavior of a free boundary in the phase field model (Carnegie–Mellon Research Report Number 82-5, 1982).
8. G. Caginalp, *Lecture Notes in Physics*, Applications of Field Theory to Statistical Mechanics, L. Garrido, ed. (Springer, Berlin, 1984), p. 216
9. R. Almgren, Second-order phase field asymptotics for unequal conductivities, *SIAM J. Appl. Math*. **59**:2086 (1999); See also, S. Hariharan and G. W. Young, Comparison of asymptotic solutions of a phase-field model to a sharp-interface model, *SIAM J. Appl. Math*. **62**:244 (2001)
10. Y. Kim, N. Provatas, N. Goldenfeld, and J. Dantzig, Universal dynamics of phase-field models for dendrite growth, *Phys. Rev. E* **59**:2546 (1999)
11. G. Caginalp, Material instabilities in continuum problems and related mathematical problems, Heriot–Watt Symposium (1985–1986), J. Ball, ed. (Oxford Science Publications, Oxford, England, 1988), p. 35
12. G. Caginalp, An analysis of a phase field mdel of a free boundary, *Arch. Rational Mech. Anal*. **92**:205 (1986)
13. G. Caginalp and E. A. Socolovsky, Efficient computation of a sharp interface by spreading via phase field methods, *Appl. Math. Lett*. **2**:117 (1989)
14. T. Abel, E. Brener, and H. M. Krumbhaar. Three-dimensional growth morphologies in diffusion-controlled channel growth, *Phys. Rev. E* **55**:7789 (1997)
15. A. Karma and W-J. Rappel, Quantitative phase-field modeling of dendritic growth in two and three dimensions, *Phys. Rev. E* **57**:4323 (1998)
16. A. Karma, Y. H. Lee, and M. Plapp, Three-dimensional dendrite-tip morphology at low undercooling, *Phys. Rev. E* **61**:3996 (2000)
17. N. Provatas, N. Goldenfeld, J. Dandtzig, J. C. Lacombe, A. Lupelescu, M. B. Koss, M. E. Glicksman, and R. Almgreen, Crossover scaling in dendritic evolution at low undercooling, *Phys. Rev. Lett*. **82**:4496 (1999)
18. J. A. Warner, R. Kobayahsi, and W. C. Carter, Modeling grain boundaries using a phase-field technique, *J. Cryst. Growth* **211**:18 (2000)
19. N. Provatas, N. Goldenfeld, and J. Dandtzig, Adaptive mesh refinement computation of solidification microstructures using dynamic data structure, *J. Comp. Phys* **148**:265 (1999)
20. S-L. Wang, R. F. Sekerka, A. A. Wheeler, B. F. Murray, S. R. Coriell, J. Brown, and G. B. McFAdden, Thermodynamically-consistent phase-field models for soldification, *Phys. D* **69**:189 (1993)
21. L. L. Regel, W. R. Wilcox, D. Popov, and F. C. Li, Influence of freezing rate oscillations and convection on eutectic microstructure, *Acta Astronautica* **48**:101 (2001)

22. G. Caginalp and X. Chen, *On the Evolution of Phase Boundaries*, E. Gurtin and G. McFadden, eds. (Springer-Verlag, New-York, Vol. 1, 1992)
23. M. E. Glicksman, M. B. Koss, and E. A. Winsa, Dendritic growth velocities in microgravity, *Phys. Rev. Lett.* **73**:573 (1994)
24. M. E. Glicksman and N. B. Singh, Effects of crystal-melt interfacial energy anisotropy on dendritic morphology and growth kinetics, *J. Cryst. Growth* **98**:207 (1989)
25. G. Caginalp, The role of microscopic anisotropy in macroscopic behavior of a phase boundary, *Ann. Phys.* **172**:136 (1986)
26. G. D. Smith, *Numerical Solution of PDE* (Oxford Applied Mathematics and Computing Science Series, 1985)
27. M. E. Glicksman, R. J. Schaefer, and J. D. Ayers, Dendritic growth-a test of theory, *Met. Mat. Trans. A* **7**:1747 (1976)
28. D. R. Kincad, J. R. Respess, D. M. Young, and R. Grimes, *Itpack2c* (University of Texas, Austin, 78712 August 1979)
29. M. Fabri and V. R Voller, The phase-field method in limit: A comparison between model potentials, *J. Comp. Physics* **130**:256 (1997)
30. R. Sekerka, Optimum stability conjecture for the role of interface kinetics in selection of dendrite operating state, *J. Cryst. Growth* **154**:377 (1995)